

MYC ASO Impedes Tumorigenesis and Elicits Oncogene Addiction in Autochthonous Transgenic Mouse Models of HCC and RCC

Renumathy Dhanasekaran,¹ Jangho Park,² Aleksey Yevtodiynko,² David I. Bellovin,² Stacey J. Adam,² Anand Rajan KD,³ Meital Gabay,² Hanan Fernando,² Julia Arzeno,² Vinodhini Arjunan,¹ Sergei Gryanzov,⁴ and Dean W. Felsher²

¹Division of Gastroenterology and Hepatology, Stanford University, Stanford, CA, USA; ²Division of Oncology, Department of Medicine and Pathology, Stanford University School of Medicine, Stanford, CA, USA; ³Department of Pathology, University of Iowa Hospitals and Clinics, Iowa City, IA, USA;; ⁴Maia Biotechnology Inc, Chicago, IL, USA

The MYC oncogene is dysregulated in most human cancers and hence is an attractive target for cancer therapy. We and others have shown experimentally in conditional transgenic mouse models that suppression of the MYC oncogene is sufficient to induce rapid and sustained tumor regression, a phenomenon known as oncogene addiction. However, it is unclear whether a therapy that targets the MYC oncogene could similarly elicit oncogene addiction. In this study, we report that using antisense oligonucleotides (ASOs) to target and reduce the expression of MYC impedes tumor progression and phenotypically elicits oncogene addiction in transgenic mouse models of MYC-driven primary hepatocellular carcinoma (HCC) and renal cell carcinoma (RCC). Quantitative image analysis of MRI was used to demonstrate the inhibition of HCC and RCC progression. After 4 weeks of drug treatment, tumors had regressed histologically. ASOs depleted MYC mRNA and protein expression in primary tumors *in vivo*, as demonstrated by real-time PCR and immunohistochemistry. Treatment with MYC ASO *in vivo*, but not with a control ASO, decreased proliferation, induced apoptosis, increased senescence, and remodeled the tumor microenvironment by recruitment of CD4⁺ T cells. Importantly, although MYC ASO reduced both mouse *Myc* and transgenic human MYC, the ASO was not associated with significant toxicity. Lastly, we demonstrate that MYC ASO inhibits the growth of human liver cancer xenografts *in vivo*. Our results illustrate that targeting MYC expression *in vivo* using ASO can suppress tumorigenesis by phenotypically eliciting both tumor-intrinsic and microenvironment hallmarks of oncogene addiction. Hence, MYC ASO therapy is a promising strategy to treat MYC-driven human cancers.

INTRODUCTION

The MYC oncogene is potentially one of the most important drug targets in cancer, as it is dysregulated in most human neoplasia. The MYC gene is at the locus 8q24.21 on chromosome 8. This region is frequently genomically amplified in human cancers. In

10,000 samples from 33 different human cancers from The Cancer Genome Atlas (TCGA) study, 28% of all tumors had genomic amplification of MYC or its paralogs.¹ Moreover, MYC is transcriptionally overexpressed in more than 50% of the tumors in 24 out of the 33 cancers they analyzed. MYC has also been shown to be commonly amplified in extrachromosomal circular DNA.^{2,3} To date, no therapies that directly target MYC exist. MYC as a nuclear transcription factor has been challenging to target using small-molecule inhibitors.⁴

MYC overexpression promotes tumorigenesis by influencing many cancer hallmarks, including inducing proliferation, blocking differentiation, promoting self-renewal, perturbing metabolism and protein biogenesis, causing genomic destabilization, and eliciting immune evasion.^{5,6} The inactivation of MYC experimentally can elicit profound tumor regression, a phenomenon that has been described as oncogene addiction. Even genetically complex tumors regress upon suppression of MYC.⁶ MYC oncogene addiction has been shown using conditional, Tet system-based transgenic mouse models in multiple types of cancer, including lymphoma,⁷ hepatocellular carcinoma,⁸ renal cell carcinoma,⁹ and osteosarcoma.¹⁰ Suppression of MYC expression in these autochthonous *in vivo* transgenic models elicits sustained tumor regression through both tumor-intrinsic and host immune-dependent mechanisms. Transgenic mouse models serve as ideal systems to test the efficacy of novel MYC therapeutics.

Synthetic oligonucleotides have complementary base pairs that target the RNA of the gene of interest and control gene expression. Antisense oligonucleotides (ASOs) can directly target MYC mRNA and have demonstrated promise in previous studies using cancer cell lines.¹¹⁻¹⁴ Deploying ASOs as cancer therapeutics has its own challenges given that their chemistry makes delivery across the cell

Received 20 March 2020; accepted 6 July 2020;
<https://doi.org/10.1016/j.omtn.2020.07.008>.

Correspondence: Dean W. Felsher, Division of Oncology, Department of Medicine and Pathology, Stanford University School of Medicine, Stanford, CA, USA.
E-mail: defelsher@stanford.edu



membrane difficult and also due to off-target effects.¹⁵ Phosphorothioate modification is a promising alteration in the backbone of the nucleic acid bases that improves stability and efficacy.¹⁶ In this study, we have used a MYC ASO with a unique lipid modification of the phosphorothioate backbone that improves drug delivery and stability.¹⁷ This MYC ASO has been shown to have potential anticancer activity in human tumor-derived cell lines.¹⁷ However, it is not known whether the ASO can be effective in aggressive primary MYC-driven tumors in immunocompetent mice, which are genetically complex and are comparable to human cancers. Using two autochthonous, conditional transgenic mouse models of MYC-driven cancers we explore the *in vivo* safety and efficacy of MYC ASO, and also decipher specific mechanisms of action.

In the present study, we report that MYC ASO can effectively inhibit MYC mRNA and protein expression *in vivo* and impede MYC-driven tumorigenesis and elicit features of oncogene addiction in conditional transgenic mouse models of MYC-driven hepatocellular carcinoma (HCC) and renal cell carcinoma (RCC) and human liver cancer xenografts. We conclude that therapeutic inhibition of MYC ASO therapy may be a treatment for human cancers.

RESULTS

Treatment with MYC ASO Effectively Inhibits MYC Expression

In Vivo

The effects of MYC ASO on tumorigenesis were studied *in vivo* using a oligo-2'-deoxyribonucleotide-containing N3' → P5' phosphoramidate. The MYC ASO 15-mer 5'-AACGTTGAGGGGCAT-3' phosphoramidate was generated complementary to the start codon region of c-MYC mRNA. The control mismatch is a 15-mer 5'-AACGAGTTGCGCCAT-3' with the same nucleoside modification. MYC ASO was administered weekly to autochthonous Tet system transgenic mouse models of MYC-driven HCC (*LAP-tTA/tet-O-MYC*)⁸ and RCC (*GGT-tTA/tet-O-MYC*)⁹ (Figure 1A).

First, we confirmed that MYC ASO but not control ASO reduced MYC protein and mRNA expression. The transgenic human c-MYC, as expected, was overexpressed in the cancer cells in the control mice (Figures 1B and 1C). Treatment with MYC ASO led to dramatic reduction in the number of nuclei that expressed MYC in the liver tumors compared to PBS-treated ($p = 0.0007$, fold change = 15.3) or control ASO-treated ($p = 0.0001$, fold change = 15.0) mice by immunohistochemistry (Figure 1B) and immunocytochemistry (Figure S1A). Similarly, MYC ASO treatment reduced MYC protein expression in RCC ($p = 0.0002$, fold change = 22.3) (Figure 1C; Figure S1B). Treatment with MYC ASO reduced transgenic human MYC mRNA expression compared to treatment with PBS ($p = 0.001$, fold change 2.7) or control ASO ($p = 0.003$, fold change 3.5). These tumors also express endogenous mouse MYC at much lower levels. Endogenous mouse MYC mRNA levels were also inhibited to a lesser degree in MYC ASO-treated mice compared to PBS-treated or control ASO-treated mice both in small tumors and large tumors (Figure 1D).

MYC ASO Inhibits MYC-Driven Tumorigenesis

Next, we examined the effects of MYC ASO versus control ASO of MYC-induced tumorigenesis. In *LAP-tTA/tet-O-MYC* transgenic mice, MYC-induced transgenic tumors were treated when tumors had reached a size of at least 50 mm³, as measured by MRI. Mice were randomized to receive intravenous delivery of either MYC ASO (30 mg/kg) ($n = 5$) or control ASO (30 mg/kg) ($n = 6$) or PBS ($n = 7$) three times a week, for 4 weeks (Figure 2A). The treatment was well tolerated and there was no significant weight loss in all three groups. Three-dimensional tumor volume assessment by MRI showed that normalized tumor volume at week 4 was significantly higher in the mice treated with PBS (mean tumor growth 196%, SEM = 60) or control mismatch ASO (mean tumor growth 86%, SEM = 63) than in the mice treated with MYC ASO (mean tumor growth 6%, SEM = 1) ($p = 0.002$ and $p = 0.01$, respectively) (Figures 2B and 2C). MYC ASO-treated transgenic mice had smaller and fewer liver tumors than did control mice when mice were sacrificed at the end of treatment (Figure 2D). Histopathologic evaluation of treated tumors showed areas of necrosis and also areas of hepatocyte-like differentiation in MYC ASO-treated tumors when compared to control tumors (Figure S2).

We next examined the effect of MYC ASO in MYC-driven RCC (*GGT-tTA/tet-O-MYC*). MYC expression in the kidney was activated at 4 weeks of age, and mice were treated either with MYC ASO ($n = 6$) or with control ASO ($n = 10$) or with PBS ($n = 8$). Weekly monitoring by MRI demonstrated that treatment with MYC ASO led to significant inhibition of RCC progression (Figures 3A and 3B). Three-dimensional volume of kidney on MRI at week 4 was significantly higher in PBS-treated (1.28 ± 0.04 mm³) and control ASO-treated mice (1.16 ± 0.03 mm³) than in MYC ASO-treated mice (0.59 ± 0.06 mm³) ($p = 0.0007$ and $p = 0.0002$, respectively). After completion of treatment, kidney weights of mice treated with PBS (mean 705 ± 45 g) or control ASO (mean, 712 ± 29 g) were significantly higher than in those treated with MYC ASO (mean, 252 ± 49 g) ($p = 0.004$ and $p = 0.0002$, respectively) (Figures 3C and 3D). Histopathologic evaluation of kidneys revealed that MYC ASO-treated mice had both fewer tumor nodules in the renal medulla and fewer dysplastic tubules (Figure 3C). Therefore, MYC ASO impedes MYC-driven tumor progression in conditional transgenic mouse models of HCC and RCC.

MYC ASO Elicits Phenotypic Features of Oncogene Addiction

We evaluated the effects of MYC ASO on tumors. The proliferative index of MYC ASO-treated but not PBS-treated ($p = 0.001$) or control ASO-treated ($p = 0.002$) HCC was reduced, as measured by phosphorylated (phospho-)histone H3 expression (Figure 4A). MYC ASO reduced Ki67-positive nuclei compared to control ASO-treated mice in both RCC and HCC (Figure S3). MYC ASO- but not control ASO-treated HCC exhibited increased apoptosis as measured by cleaved caspase-3 ($p = 0.03$) (Figure 4B). We observed previously that CD4⁺ T cells are required for tumor regression and induction of cellular senescence upon MYC inactivation.^{18,19} Consistent with our reported findings, treatment with MYC ASO but not control ASO resulted in increased CD4⁺ T cells (fold change = 2.5,

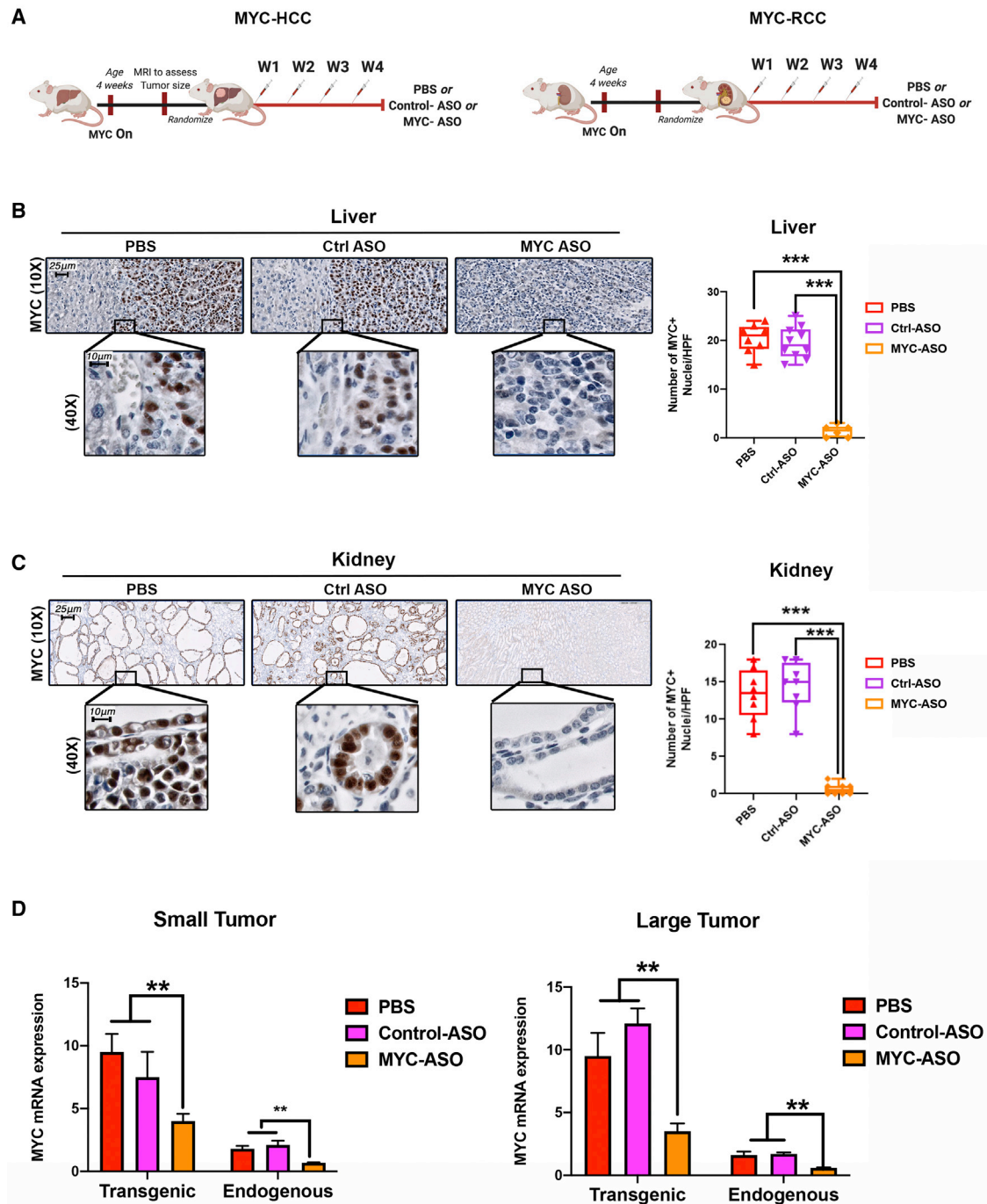


Figure 1. MYC ASO Inhibits MYC Expression in Murine Cancer

(A) Schematic of treatment of MYC-HCC and MYC-RCC with PBS or control ASO or MYC ASO. (B) Representative immunohistochemistry (IHC) images ($\times 10$ and $\times 40$) and quantification show that treatment with MYC ASO inhibits MYC protein expression in liver cancer. (C) Representative IHC images ($\times 10$ and $\times 40$) and quantification show that treatment with MYC ASO inhibits MYC protein expression in renal cell cancer. (D) Quantitative PCR for transgenic human MYC and endogenous mouse MYC in primary small and large liver tumors treated with PBS or control ASO or MYC ASO. * $p < 0.05$, ** $p < 0.01$, *** $p < 0.001$. Error bars represent standard error of mean (SEM).

$p = 0.002$) and induction of cellular senescence as measured by β -galactosidase staining (fold change = 3.8, $p = 0.002$) (Figure 4C). We did not find any difference in CD8⁺ T cell or B cell infiltration be-

tween MYC ASO- and control ASO-treated groups (Figure S4). Hence, MYC ASO is able to reverse both cell-intrinsic and immune-mediated MYC addiction.

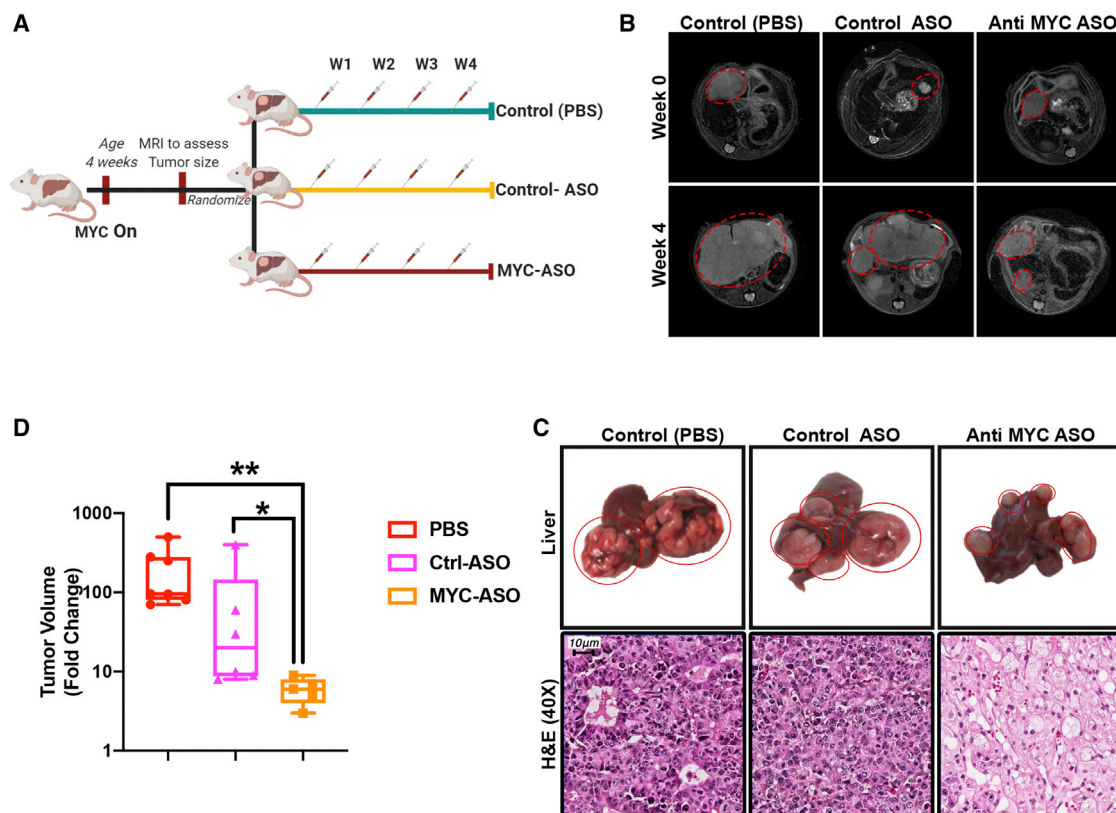


Figure 2. MYC ASO Delays Tumor Progression in a Transgenic Mouse Model of Hepatocellular Carcinoma

(A) Schematic of treatment of MYC transgenic mice with PBS or control ASO or MYC ASO. (B) Representative MRI images of liver tumors at week 0 and at week 4 of treatment. (C) Quantification to fold change in tumor volume between week 0 and week 4 in the three treatment groups. (D) Gross images and histopathology of liver tumors treated with PBS or control ASO or MYC ASO. * $p < 0.05$, *** $p < 0.001$. Error bars represent standard error of mean (SEM).

MYC ASO Treatment Is Not Associated with Morbidity, Mortality, or Toxicity

We did not observe any toxicity-related morbidity or mortality in the treatment or control groups. Treated mice did not lose more than 10% of their body weight during the 4 weeks of treatment (Figure 5A). MYC ASO decreased endogenous mouse MYC mRNA levels in non-target organs, including adrenal glands (fold change = 2.5, $p = 0.002$) and spleen (fold change = 2.6, $p = 0.001$) (Figure 5B). No change was noted in MYC mRNA levels in normal surrounding liver or in the testis. No injury was found in liver (Figure 5C), kidney (Figure 5D), spleen (Figure 5E), or testes (Figure 5F), based on histopathologic assessment and evaluation of apoptosis by cleaved caspase-3 staining (Figures 5C–5F). A pathologist performed a blinded evaluation of liver histopathology. There was no evidence of typical features of drug-induced liver injury such as lobular hepatitis, zone 3 necrosis, cholestasis, or increased apoptosis in the liver. Scattered acidophil bodies and regenerating hepatocytes were noted in all three treatment groups (Figure S5). We looked for evidence of innate immune-mediated injury in the surrounding liver and did not find a significant increase in neutrophils or macrophages infiltration upon MYC ASO treatment (Figures 5G and 5H). Also, MYC ASO treatment was not associated with significant evidence of acute neutrophilic inflamma-

tion or acute kidney injury as assessed by Kim1 staining, an established biomarker of drug-induced kidney injury²⁰ (Figure S6).

MYC ASO Inhibits Human Liver Cancer Cell Line Xenograft Growth *In Vivo*

We evaluated whether MYC ASO could inhibit the growth of the human liver cancer cell line HepG2. *In vitro*, MYC ASO but not control ASO suppressed MYC expression in HepG2 (Figure 6A) and decreased cellular proliferation (Figure 6B). To determine the *in vivo* effect of MYC ASO on HepG2-derived xenografts, we treated tumor-bearing mice with MYC ASO ($n = 9$) or control ASO ($n = 4$) or PBS ($n = 8$) (Figure 6C). MYC ASO (mean, 9 mm³) treatment led to a significant reduction in HepG2 xenograft growth compared to PBS (mean, 43 mm³) or control ASO (mean, 35 mm³) ($p < 0.001$) (Figures 6C and 6D). Hence, MYC ASO blocks MYC expression and reduces tumor growth in human liver cancer xenografts.

DISCUSSION

MYC is the most commonly activated oncogene in human cancer, but it has yet to be directly targeted therapeutically.⁴ In this study, we show that a MYC ASO can be used to suppress MYC expression in

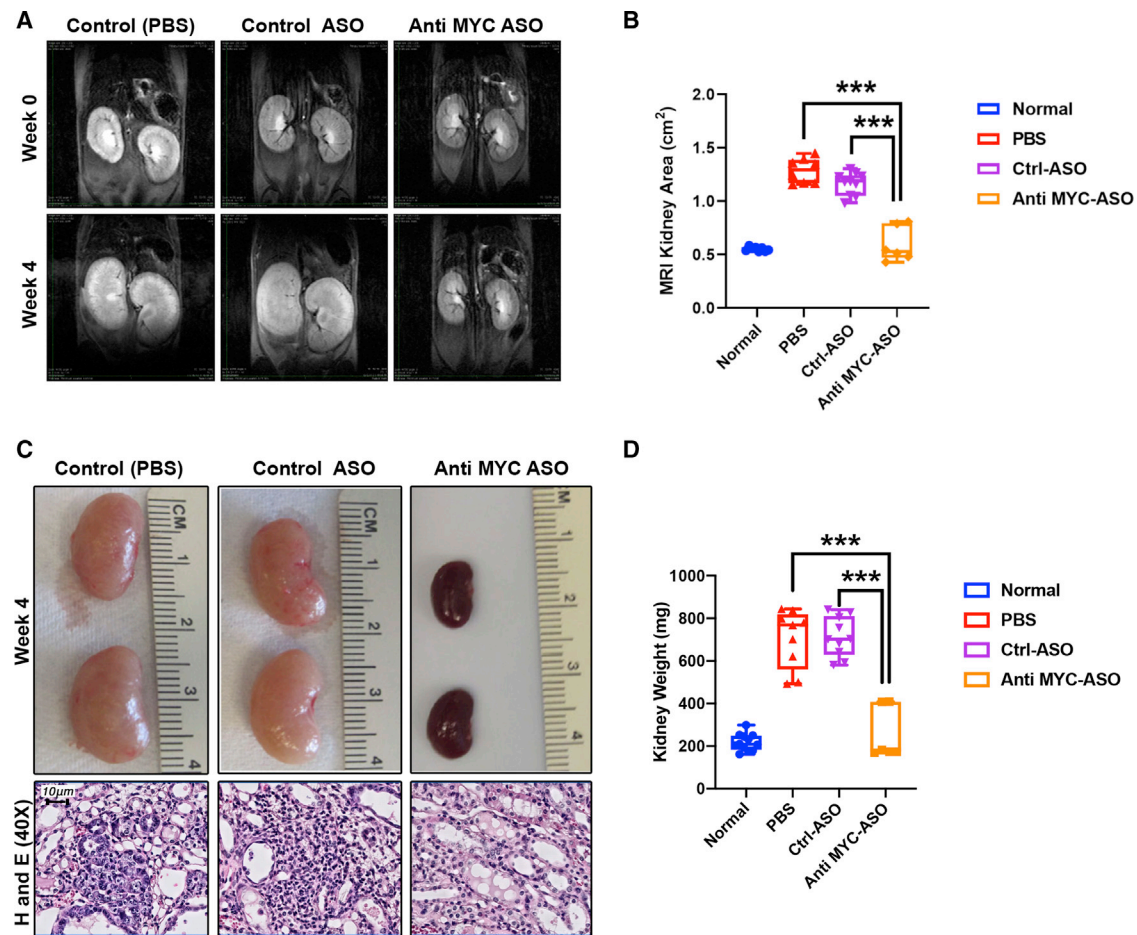


Figure 3. MYC ASO Delays Tumor Progression in a Transgenic Mouse Model of Renal Cell Carcinoma

(A) Representative MRI images of mice with MYC-driven kidney cancers at week 0 and at week 4 of treatment. (B) Quantification to fold change in kidney size between week 0 and week 4 in the three treatment groups. (C) Gross images and histopathology of kidney tumors treated with PBS or control ASO or MYC ASO. (D) Comparison of kidney weights at the time of euthanasia between the three treatment groups. * $p < 0.05$, *** $p < 0.001$. Error bars represent standard error of mean (SEM).

autochthonous transgenic mouse models of MYC-driven HCC, RCC, and xenograft tumors and elicit phenotypic features of oncogene addiction. Importantly, MYC ASO reduced both endogenous mouse Myc and human MYC but was not associated with significant toxicity.

Oligonucleotide phosphoramidates such as thio-phosphoramidates conjugated with lipid groups are cell-permeable and have shown high target-specific activity.¹⁷ The nucleic acid backbone structure of the MYC ASO we have used in the present study provides resistance to intracellular nucleases, improves stability, and improves target affinity. Our observations suggest that MYC ASO¹² can be used therapeutically to suppress MYC-driven tumorigenesis *in vivo* in autochthonous transgenic mouse models of MYC-driven HCC and RCC, and in a xenograft model of human liver cancer. MYC ASO reduced MYC protein and mRNA expression in tumors and was associated with many of the phenotypic features of MYC-associated oncogene addiction, including proliferative arrest, apoptosis, dif-

ferentiation, senescence, and increased CD4⁺ T cell infiltration. MYC ASOs did not appear to be associated with toxicity. We conclude that MYC ASOs may be an effective strategy to treat MYC-driven human cancers.

Our study demonstrates the efficacy of MYC ASO *in vivo* using two transgenic mouse models of aggressive MYC-driven primary cancers and in a human xenograft. Previous studies in prostate cancer¹¹ and leukemia-derived cell lines¹² had suggested that MYC ASO can be effective in cancer therapy. The *in vivo* model systems used in this study have several distinct advantages and make our findings more relevant to human cancers. We have evaluated the ASO in autochthonous transgenic mice, which has enabled us to confirm efficient ASO delivery to primary tumors arising orthotopically in their native organs. Moreover, the primary transgenic mice have an intact immune system, thus allowing us to evaluate the changes elicited by the ASO in the cognate immune microenvironment.

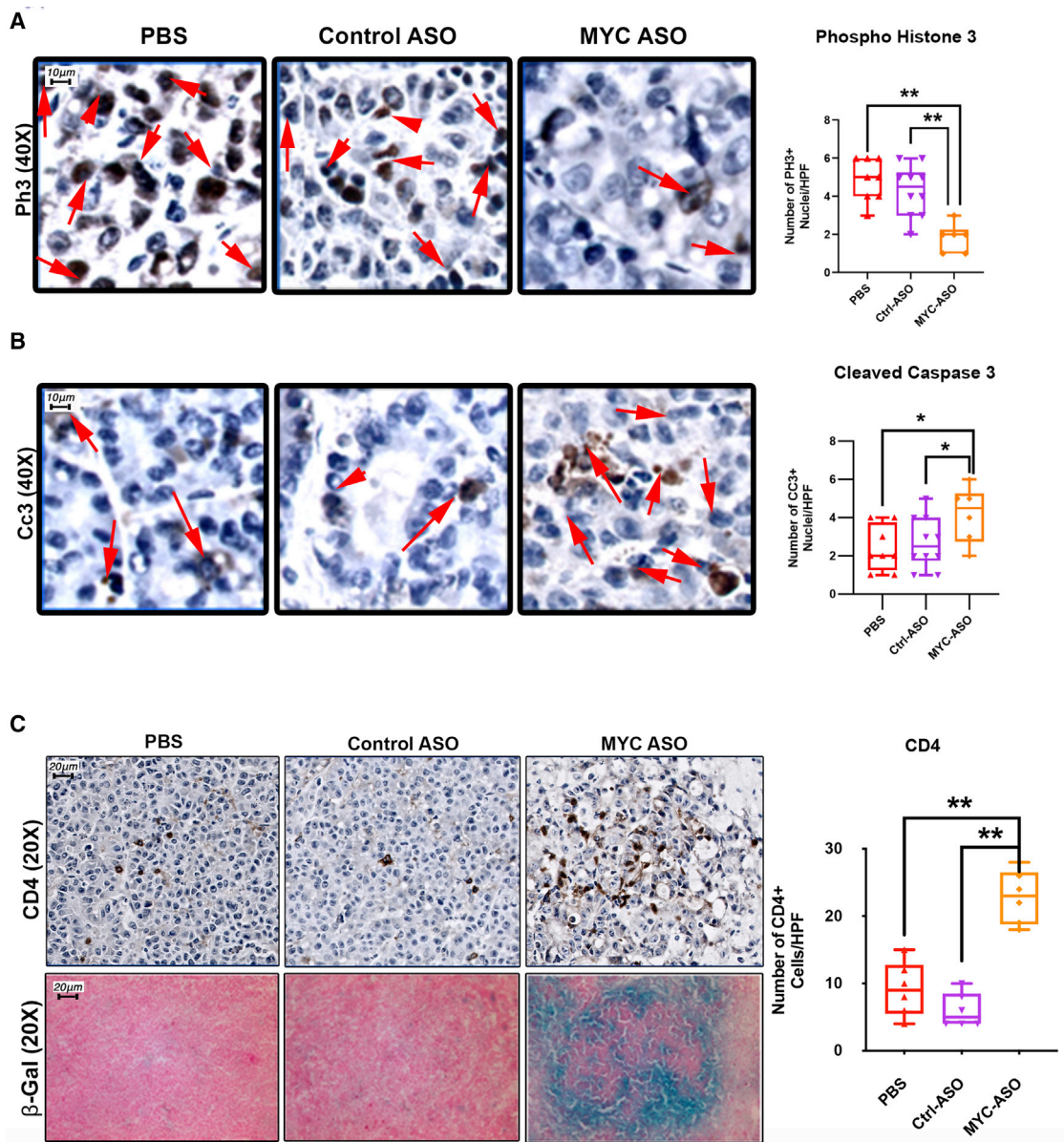


Figure 4. Mechanism of Action of MYC ASO

(A) Liver tumors treated with MYC ASO demonstrate a lower proliferative index as measured by phospho-histone H3 staining. Quantification of CC3 staining in primary liver tumors. (B) Cleaved caspase-3 staining is higher in liver tumors treated with MYC ASO than PBS or control ASO treated. Quantification of CC3 staining in primary liver tumors. (C) IHC shows increased infiltration of CD4⁺ T cells in MYC ASO-treated tumors compared to PBS- or control ASO-treated tumors. Treatment with MYC ASO is associated with increased expression of the senescence marker β -galactosidase. * $p < 0.05$, ** $p < 0.01$, *** $p < 0.001$. Error bars represent standard error of mean (SEM).

Previously, we and others have shown that complete suppression of MYC transgene expression results in dramatic tumor regression in conditional transgenic mouse models.^{7-10,18} In this study, we used MYC ASO to significantly suppress MYC expression in primary liver and kidney tumors *in vivo* and evaluate whether the oncogene addiction observed in transgenic models can be triggered by this therapeutic intervention. We demonstrate that even the partial MYC suppression with the MYC ASO *in vivo* in transgenic mouse models and human

liver cancer xenografts dramatically reduced tumor growth. We were able to indeed elicit many of the phenotypic features of oncogene addiction for both tumor cell-intrinsic-like proliferative arrest, differentiation, and apoptosis and host-dependent mechanisms such as CD4⁺ T cell infiltration and the associated induction of senescence, as reported in our previous work.¹⁹ Longer term follow-up after completion of treatment will be needed to further evaluate the role of CD4⁺ T cells in tissue remodeling and elimination of minimal residual disease.

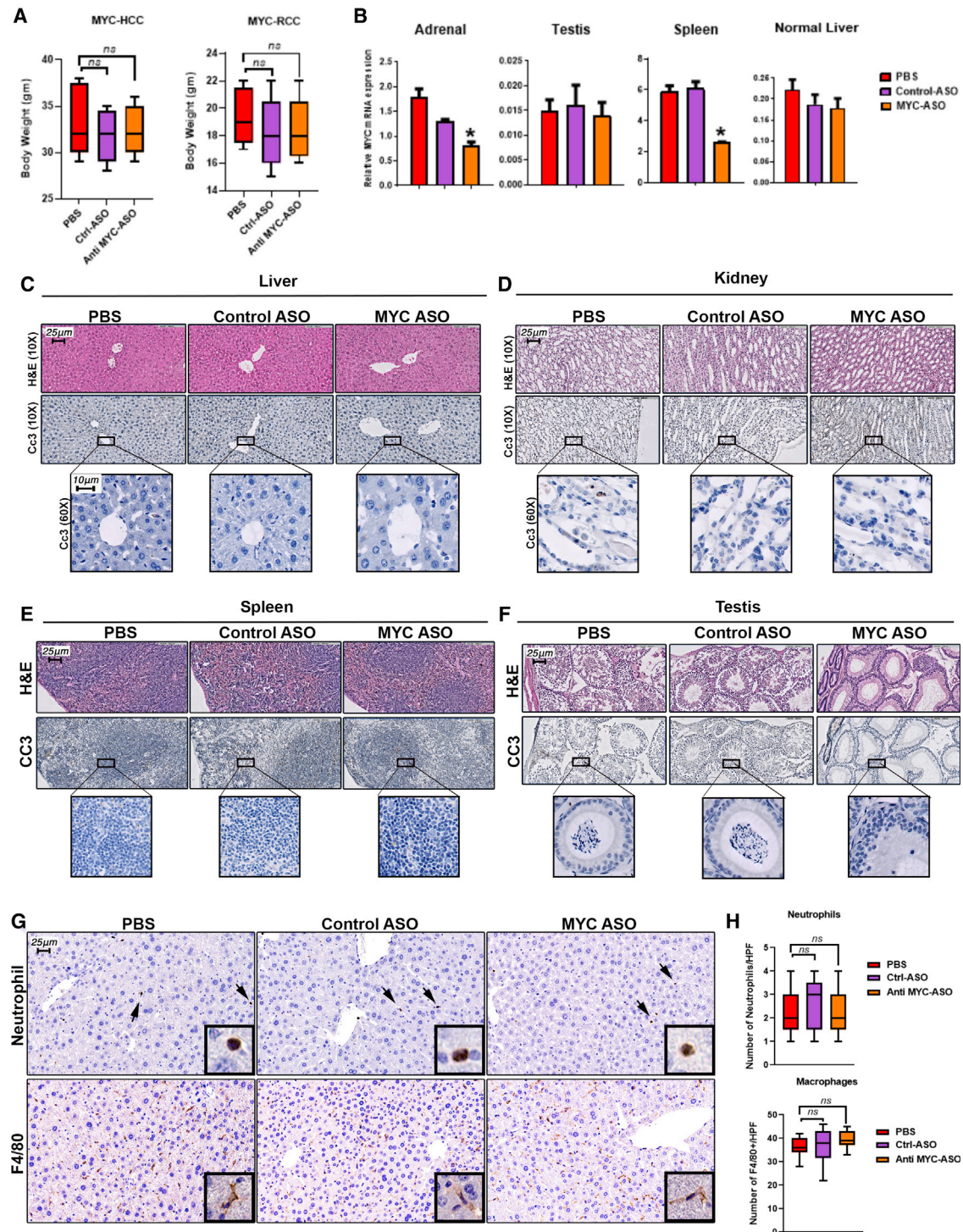


Figure 5. ASO-Mediated MYC Knockdown Is Well Tolerated in Mice

(A) Body weight of MYC-driven HCC and RCC treated with PBS, control ASO, or MYC ASO. (B) Quantitative PCR for endogenous mouse MYC expression in non-target organs such as the adrenal glands, testes, spleen, and normal liver in transgenic kidney cancer mice treated with PBS or control ASO or MYC ASO. (C–F) Histopathology and immunohistochemical staining for cleaved caspase-3 in mouse liver (C), kidney (D), spleen (E), and testis (F) of transgenic mice treated with PBS or control ASO or MYC ASO. (G) IHC for neutrophils and macrophages (F4/80) in three treatment groups. (H) Graphs show quantification of IHC staining. Error bars represent standard error of mean (SEM).

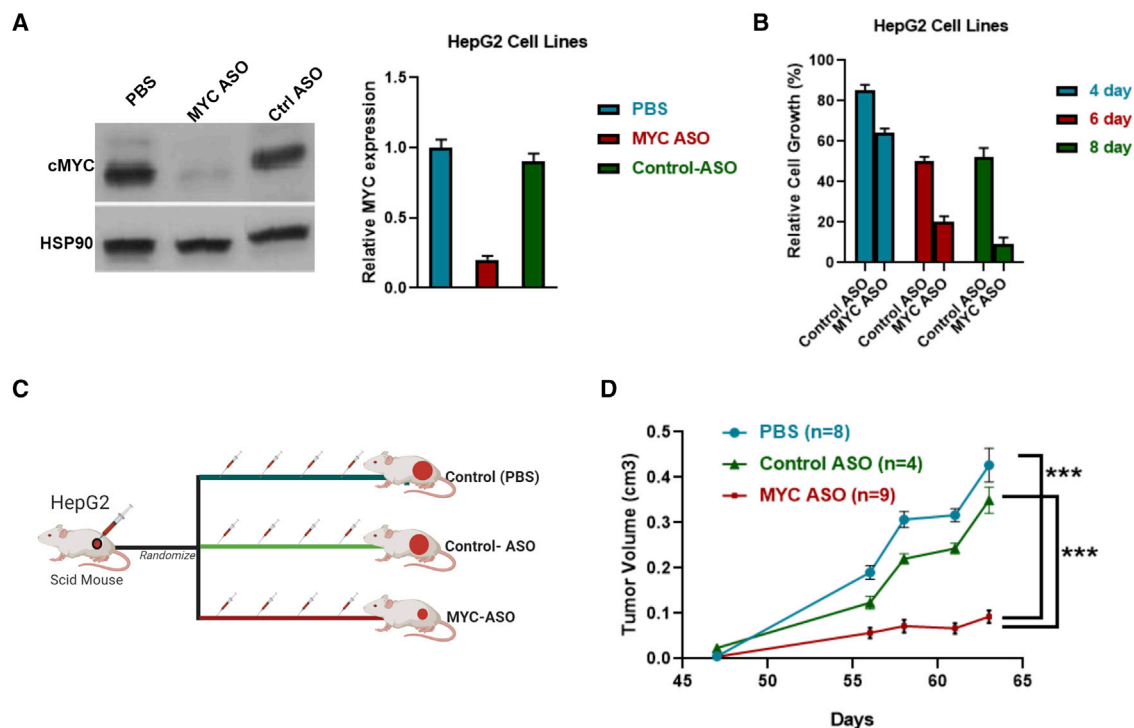


Figure 6. MYC ASO Inhibits Growth of Human Liver Cancer Xenograft

(A) Immunoblotting shows that treatment of HepG2 cells with MYC ASO leads to decreased MYC expression compared to PBS treatment or control ASO treatment. Quantification of immunoblots is shown. (B) MTT assay to measure cell growth of HepG2 upon *in vitro* treatment with MYC ASO or control at day 4, day 6, or day 8. (C) Experimental scheme for treatment of subcutaneous xenografts of HepG2 in immunocompromised mice. *** $p < 0.001$. (D) *In vivo* growth of HepG2 xenografts upon treatment with PBS or control ASO or MYC ASO. * $p < 0.05$, ** $p < 0.01$, *** $p < 0.001$. Error bars represent standard error of mean (SEM).

MYC ASO was not associated with significant morbidity or mortality in the treated mice. The ASO had specificity against both the transgenic human MYC and the endogenous murine Myc. Notably, endogenous Myc levels were reduced by more than 2-fold in off-target organs such as the adrenal glands and spleen, but this was not associated with toxicity. Our findings are consistent with the experimental observation that while MYC knockout (*Myc*^{-/-}) is embryonic lethal, MYC haploinsufficient (*Myc*^{+/-}) mice are viable and indeed have a survival advantage.²¹ Similarly, the toxicity induced by MYC suppression through omo-MYC has been shown to be easily reversible upon MYC restoration.²² We did not find any evidence for immune activation by the ASO, likely because the oligonucleotide is a short sequence and does not contain CpG oligodeoxynucleotide motifs. More detailed evaluations of short-term and long-term cytokine profiles are needed in future studies.

We conclude that MYC ASO can elicit features associated with oncogene addiction and reduce tumor growth without inducing toxicity. Our results support the concept that targeting MYC directly may serve as a tumor-agnostic treatment strategy across multiple human cancers.

MATERIALS AND METHODS

Transgenic Mice

All procedures and housing of animals were in accordance with Stanford's Administrative Panel on Laboratory Animal Care (APLAC)

protocols. Liver-specific *LAP-tTa/tet-O-MYC* transgenic lines and kidney-specific *GGT-tTa/tet-O-MYC* have previously been described.^{8,9} Mice received 0.1 mg/mL of doxycycline (Sigma) via drinking water until 4 weeks of age and then taken off doxycycline. The mice were imaged by MRI to screen for tumors and euthanized after completion of treatment.

Antisense Oligonucleotide Drug Delivery

The antisense oligonucleotides used in this study were synthesized by Geron (Menlo Park, CA, USA). MYC ASO or control ASO was injected with a dose of 30 mg/kg intravenously. Control mice were treated with PBS. The sequence of the MYC ASO is 5'-AACGTTGAGGGGCAT-3' phosphoramidate, and the mismatch oligonucleotide 15-mer is 5'-AACGAGTTGCGCCAT-3'.

Small Animal Imaging

Animals were imaged using the Bruker 7T MRI (Agilent Technologies conversion) with a 40-mm Varian Millipede RF coil and ParaVision (PV6.01) software at the Stanford Center for Innovation in In Vivo Imaging (SCI3). Animals were anesthetized by inhalation with 1%–3% isoflurane mixed with medical-grade oxygen in a knock-down box in compliance with the APLAC protocols. The mice were then immobilized onto a mouse bed insert and loaded into the MRI. Their respiration rate and body temperature were monitored

Table 1. Antibodies Used in This Work

Reagent Type (Species) or Resource	Designation	Source or Reference	Identifiers	Additional Information
Antibody	MYC (rabbit monoclonal)	Epitomics	RRID:AB_11000313	IHC (1:150), IF (1:150), WB (1:1,000)
Antibody	phospho-histone H3 (rabbit, polyclonal)	Cell Signaling Technology	RRID:AB_331535	IHC (1:100)
Antibody	cleaved caspase-3 (rabbit)	Cell Signaling Technology	RRID:AB_2341188	IHC (1:100)
Antibody	Ki67	Abcam	ab15580	IF 1:500
Antibody	CD4 (mouse, monoclonal)	Abcam	RRID:AB_2686917	IHC (1:1,000)
Antibody	CD8	Abcam	ab4055	IHC
Antibody	CD19	Cell Signaling Technology	D4V4B	IHC
Antibody	neutrophil	Abcam	ab2557	IHC
Antibody	F4/80	Thermo Fisher Scientific	MF48000	IHC
Antibody	Tim-1 (Kim1)	Abcam	ab47635	IHC

IHC, immunohistochemistry; IF, immunofluorescence; WB, western blot.

with respiratory and temperature probes through PC-SAM software. Their body temperature was kept constant by a heater, and their respiration was kept at a safe level by adjusting the isoflurane. Tumors were detected with a respiration triggered T2-weighted 3D turbo spin-echo sequence (repetition time [TR]/echo time [TE] 3,000/205 ms; voxel size, 0.22 mm). The isotropic voxel size in all directions allowed for a high-plane and across-plane resolution and allowed us to precisely determine the location and size of individual tumor nodules. The mice were imaged approximately every 7 days. After the mice were imaged, they were allowed to recover in a warmed recovery box before being placed back into their housing. Digital Imaging and Communications in Medicine (DICOM) images were quantified using OsiriX DICOM Viewer software (OsiriX, UCLA, and Los Angeles, CA, USA).

Cell Culture and *In Vitro* Cell Viability Assay

HepG2 cell lines (ATCC, Rockville, MD, USA) were cultivated in DMEM supplemented with 10% fetal bovine serum and maintained at 37°C (95% air, 5% CO₂) and cultured as per the ATCC guidelines. The effects of MYC ASO on cell viability were determined by a microculture tetrazolium technique (MTT) assay. Cells were seeded (1 × 10⁵ cells/well) and treated with control ASO or MYC ASO (concentration of 1 μM) for 8 days. Following treatment, cells were incubated with MTT (5 mg/mL in PBS) at 37°C for 4 h before DMSO was added to dissolve the formazan crystals, and the absorbance of each well was determined at 492 nm on an automated microplate reader. Cellular viability was measured after 4, 6, or 8 days of treatment.

Human Cell Line Xenograft Generation and *In Vivo* Treatment

HepG2 cells were grown in culture as mentioned above. Cells (5 × 10⁶ cells/mouse) were injected subcutaneously in the flank of non-severe combined immunodeficiency (SCID)-gamma (NSG) mice, which were 4–6 weeks old. Mice were observed daily until a small tumor was palpable. Mice were randomized to receive PBS or control ASO or MYC ASO at 30 mg/kg intravenously. Mice were monitored closely and tumor growth was measured by calipers. The results were converted to tumor volume (mm³) by the formula (length × width²) × 1/2.

Immunohistochemistry and Immunofluorescence

Tissues were fixed in 4% paraformaldehyde. The fixed tissues were then embedded in paraffin and sectioned. Sections were deparaffinized through incubation in xylene and rehydrated through graded incubation in ethanol. The sections were steamed in Dako antigen retrieval solution for 45 min to unmask epitopes. The sections were then immunostained overnight at 4°C with MYC (1:150, Epitomics), phospho-histone H3 (1:200, Cell Signaling Technology), cleaved caspase-3 (1:100, Cell Signaling Technology), Ki67 (Abcam ab15580), β-galactosidase (Sigma CS0030), and Cd4 (1:1,000, Abcam) and washed with PBS. The sections were then incubated with biotinylated anti-mouse, anti-rabbit, or anti-mouse secondary antibody (1:300) for 30 min at room temperature (for antibodies, see Table 1). The sections were washed with PBS and incubated with ABC reagent for 30 min at room temperature (1:300, Vectastain ABC kit, Vector Laboratories). The sections were stained with 3,3'-diaminobenzidine (DAB), counterstained with hematoxylin, and mounted with Permount. The stained sections were scanned and imaged on a digital pathology slide scanner (Philips). The scanned sections were quantified using ImageJ software (NIH).

SUPPLEMENTAL INFORMATION

Supplemental Information can be found online at <https://doi.org/10.1016/j.omtn.2020.07.008>.

AUTHOR CONTRIBUTIONS

Conceptualization, R.D., D.I.B., A.Y., S.J.A., M.G., H.F., J.A., V.A., S.G., and D.W.F.; Visualization, R.D.; Methodology, R.D., J.P., D.I.B., A.Y., S.J.A., M.G., H.F., J.A., V.A., and A.R.K.; Investigation, R.D., J.P., D.I.B., A.Y., S.J.A., M.G., H.F., J.A., V.A., and A.R.K.; Formal Analysis, A.R.K.; Writing – Original Draft, R.D. and J.P.; Writing – Review & Editing, S.G. and D.W.F.; Supervision, S.G. and D.W.F.; Resources, D.W.F.; Project Administration, D.W.F.; Funding Acquisition, D.W.F.

CONFLICTS OF INTEREST

This work was supported in part by funding from Geron, USA. Otherwise, the authors declare no competing interests.

ACKNOWLEDGMENTS

The work was partially supported by Geron Corp. and by National Institutes of Health (NIH) grants CA208735, R01 CA184384, CA170378, and U01 CA188383 from the National Cancer Institute (NCI) (to D.F.) and National Institutes of Health (NIH) grant CA222676 from the National Cancer Institute (NCI) (to R.D.), as well as by an American College of Gastroenterology Junior Faculty Career Development Grant (to R.D.).

REFERENCES

- Schaub, F.X., Dhankani, V., Berger, A.C., Trivedi, M., Richardson, A.B., Shaw, R., Zhao, W., Zhang, X., Ventura, A., Liu, Y., et al.; Cancer Genome Atlas Network (2018). Pan-cancer alterations of the MYC oncogene and its proximal network across The Cancer Genome Atlas. *Cell Syst.* *6*, 282–300.e2.
- Turner, K.M., Deshpande, V., Beyter, D., Koga, T., Rusert, J., Lee, C., Li, B., Arden, K., Ren, B., Nathanson, D.A., et al. (2017). Extrachromosomal oncogene amplification drives tumour evolution and genetic heterogeneity. *Nature* *543*, 122–125.
- Verhaak, R.G.W., Bafna, V., and Mischel, P.S. (2019). Extrachromosomal oncogene amplification in tumour pathogenesis and evolution. *Nat. Rev. Cancer* *19*, 283–288.
- Dang, C.V., Reddy, E.P., Shokat, K.M., and Soucek, L. (2017). Drugging the “undruggable” cancer targets. *Nat. Rev. Cancer* *17*, 502–508.
- Dang, C.V. (2012). MYC on the path to cancer. *Cell* *149*, 22–35.
- Gabay, M., Li, Y., and Felsher, D.W. (2014). MYC activation is a hallmark of cancer initiation and maintenance. *Cold Spring Harb. Perspect. Med.* *4*, a014241.
- Felsher, D.W., and Bishop, J.M. (1999). Reversible tumorigenesis by MYC in hematopoietic lineages. *Mol. Cell* *4*, 199–207.
- Shachaf, C.M., Kopelman, A.M., Arvanitis, C., Karlsson, A., Beer, S., Mandl, S., Bachmann, M.H., Borowsky, A.D., Ruebner, B., Cardiff, R.D., et al. (2004). MYC inactivation uncovers pluripotent differentiation and tumour dormancy in hepatocellular cancer. *Nature* *431*, 1112–1117.
- Shroff, E.H., Eberlin, L.S., Dang, V.M., Gouw, A.M., Gabay, M., Adam, S.J., Belov, D.I., Tran, P.T., Philbrick, W.M., Garcia-Ocana, A., et al. (2015). MYC oncogene overexpression drives renal cell carcinoma in a mouse model through glutamine metabolism. *Proc. Natl. Acad. Sci. USA* *112*, 6539–6544.
- Jain, M., Arvanitis, C., Chu, K., Dewey, W., Leonhardt, E., Trinh, M., Sundberg, C.D., Bishop, J.M., and Felsher, D.W. (2002). Sustained loss of a neoplastic phenotype by brief inactivation of MYC. *Science* *297*, 102–104.
- Balaji, K.C., Koul, H., Mitra, S., Maramba, C., Reddy, P., Menon, M., Malhotra, R.K., and Laxmanan, S. (1997). Antiproliferative effects of c-myc antisense oligonucleotide in prostate cancer cells: a novel therapy in prostate cancer. *Urology* *50*, 1007–1015.
- Skorski, T., Perrotti, D., Nieborowska-Skorska, M., Gryaznov, S., and Calabretta, B. (1997). Antileukemia effect of c-myc N3' → P5' phosphoramidate antisense oligonucleotides in vivo. *Proc. Natl. Acad. Sci. USA* *94*, 3966–3971.
- Iversen, P.L., Arora, V., Acker, A.J., Mason, D.H., and Devi, G.R. (2003). Efficacy of antisense morpholino oligomer targeted to c-myc in prostate cancer xenograft murine model and a phase I safety study in humans. *Clin. Cancer Res.* *9*, 2510–2519.
- Sekhon, H.S., London, C.A., Sekhon, M., Iversen, P.L., and Devi, G.R. (2008). c-MYC antisense phosphorodiamidate morpholino oligomer inhibits lung metastasis in a murine tumor model. *Lung Cancer* *60*, 347–354.
- Shen, X., and Corey, D.R. (2018). Chemistry, mechanism and clinical status of antisense oligonucleotides and duplex RNAs. *Nucleic Acids Res.* *46*, 1584–1600.
- Sharma, V.K., and Watts, J.K. (2015). Oligonucleotide therapeutics: chemistry, delivery and clinical progress. *Future Med. Chem.* *7*, 2221–2242.
- Gryaznov, S.M. (2010). Oligonucleotide N3' → P5' phosphoramidates and thio-phosphoramidates as potential therapeutic agents. *Chem. Biodivers.* *7*, 477–493.
- Wu, C.-H., van Riggelen, J., Yetil, A., Fan, A.C., Bachireddy, P., and Felsher, D.W. (2007). Cellular senescence is an important mechanism of tumor regression upon c-Myc inactivation. *Proc. Natl. Acad. Sci. USA* *104*, 13028–13033.
- Rakhra, K., Bachireddy, P., Zabuawala, T., Zeiser, R., Xu, L., Kopelman, A., Fan, A.C., Yang, Q., Braunstein, L., Crosby, E., et al. (2010). CD4⁺ T cells contribute to the remodeling of the microenvironment required for sustained tumor regression upon oncogene inactivation. *Cancer Cell* *18*, 485–498.
- Griffin, B.R., Faubel, S., and Edelstein, C.L. (2019). Biomarkers of drug-induced kidney toxicity. *Ther. Drug Monit.* *41*, 213–226.
- Hofmann, J.W., Zhao, X., De Cecco, M., Peterson, A.L., Pagliaroli, L., Manivannan, J., Hubbard, G.B., Ikeno, Y., Zhang, Y., Feng, B., et al. (2015). Reduced expression of MYC increases longevity and enhances healthspan. *Cell* *160*, 477–488.
- Soucek, L., Whitfield, J., Martins, C.P., Finch, A.J., Murphy, D.J., Sodik, N.M., Karnezis, A.N., Swigart, L.B., Nasi, S., and Evan, G.I. (2008). Modelling Myc inhibition as a cancer therapy. *Nature* *455*, 679–683.